

CONSISTENT INSERTION OF BOND-SLIP INTO BEAM FIBER ELEMENTS FOR BIAXIAL BENDING

GIORIGO MONTI¹ AND ENRICO SPACONE²

SUMMARY

In this paper a new reinforced concrete beam finite element that explicitly accounts for the bond-slip between the reinforcing bars and the surrounding concrete is presented. The element formulation combines the fiber section model with the finite element model of a reinforcing bar with continuous slip. The section model retains the plane section assumption, but the steel fiber strains are computed as the sum of two contributions: the rebar deformation and the anchorage slip. The proposed finite element includes material nonlinearities in the concrete, steel and bond-slip constitutive laws. The formulation applies to both monotonic and cyclic loads, and is therefore suitable for the seismic analysis of reinforced concrete structures in which the rebar slips must be accounted for. Since each longitudinal steel bar is monitored separately, the model applies to any cross sectional shape and extends to both uniaxial and biaxial bending. First, the theoretical framework is presented, then a correlation study with an experimental test on a cantilever column with circular cross section is discussed. This study shows that the prediction with the new model is in good agreement with the experimental test, while the original fiber model with perfect bond overestimates the hysteretic energy dissipated during the loading cycles.

INTRODUCTION

By modelling the response of single embedded bars and r.c. members with bars anchored in the footings, it can be noticed that bond-slip affects the local behavior of the bar. As a consequence of this local behavior, the base moment-curvature diagram is equally affected, even though to a lesser extent, but it can be observed that the request of ductility is slightly higher than in the case with full bond. Minor differences are observed in the force-displacement diagram, because global quantities are less sensitive to local modifications. Nonetheless, also in this case the initial stiffness is lower. This may have meaningful effects on more complex structural systems, whose response to dynamic actions is stiffness-driven.

Notwithstanding the recognized importance of these effects, in the analysis of reinforced concrete structures, perfect bond is usually assumed between the rebars and the surrounding concrete. This is true for low load levels, whereas, as the load increases, cracking as well as breaking of bond unavoidably occurs and bond-slip takes place in the beam. Near the cracks, high bond stresses develop at the steel-concrete interface causing relative displacements between concrete and reinforcement. In particular, two effects are significant: a) an increase in stiffness in the regions between two adjacent cracks, and b) an increase of flexibility at the member ends, due to the pullout of the rebars at the interface with either other framing elements or the footings. Similar drops in stiffness may also be caused by insufficient lap splices. These effects become particularly important and complex under seismic loading conditions, when bond deteriorates due to large strains and damage caused by load reversals.

The formulation of the beam element including the bond-slip effect derives from that originally proposed by Spacone *et al.* (1996), with the insertion of the continuous bond element developed by Monti *et al.* (1997). The framework of the fiber section state determination is retained, while a new approach is proposed for computing the rebar stress and stiffness that include the effects of slip. The response of the bar is lumped at the fiber level. The steel fiber strain is given by the sum of the effects of the rebar deformation and the anchorage slip. The end

¹ Associate Professor, Università La Sapienza di Roma, Via Gramsci, 53 – 00197 Rome, Italy - E-mail: monti@uniroma1.it

² Assistant Professor, University of Colorado, Boulder, CO 80309-0428, USA - E-mail: spacone@colorado.edu

slip is also calculated, to give an estimate of the crack width. Also the anchorage length outside the element, in either a structural joint or a footing, is accounted for. This makes the new model particularly easy to implement into any existing fiber beam finite element. This approach allows to consistently account for bond-slip also in biaxial bending conditions.

REINFORCED CONCRETE FIBER BEAM ELEMENT WITH BOND-SLIP

In fiber beam finite elements, the state determination is carried out at three levels: element, section and fiber. At all three levels, the problem is the same: determine the forces (or stresses) and stiffness corresponding to prescribed deformations. In particular, the section state determination computes the section axial force and bending moment corresponding to prescribed section deformations, namely the average axial strain $\bar{\epsilon}$ and the section curvature κ . The discussion is limited here to the uniaxial bending case, but extension to the biaxial case is straightforward.

From the plane sections assumption, the strain at a fiber located at a distance y from the reference axis is:

$$\epsilon = \bar{\epsilon} + \kappa y \quad (1)$$

When perfect bond is assumed between concrete and steel rebar, concrete and steel fibers located at the same depth y have the same strain:

$$\epsilon_s = \epsilon_c = \epsilon = \bar{\epsilon} + \kappa y \quad (2)$$

This assumption is removed in order to include the effects of bond-slip.

Because of the numerical integration used to solve the element integrals, the beam element is modeled as a set of adjacent slices that are connected in series. The element response is the weighted sum of the responses of each slice. If one considers a beam element of length L_{beam} , the length of each slice is $L_{IP} = w_{IP} L_{beam}$. The slice length L_{IP} is a function of the integration scheme, the number of integration points and thus the weight w_{IP} pertaining to the integration point IP . Each slice can be considered as a parallel system made of two components, steel and concrete. From the assumption of perfect bond, the slice and its components have the same elongation \bar{d} and rotation φ

$$\begin{cases} \bar{d} = \bar{d}_c = \bar{d}_s \\ \varphi = \varphi_c = \varphi_s \end{cases} \quad (3)$$

in which \bar{d}_c, \bar{d}_s and φ_c, φ_s are the slice elongations and rotations in the concrete and steel components, respectively. The slice is basically a finite length of beam element L_{IP} with constant deformations. These are the axial strain $\bar{\epsilon}$ and the curvature κ of the integration point IP , therefore:

$$\begin{cases} \bar{d} = \bar{\epsilon} L_{IP} \\ \varphi = \kappa L_{IP} \end{cases} \quad (4)$$

With this notation, the compatibility condition of Eq. (2) can be expressed in terms of concrete and steel displacements. The elongation of a fiber at distance y from the reference axis can be written:

$$u(y) = u_c = u_s = \bar{d} + \varphi y \quad (5)$$

From Eqs. (1) and (4) the strain distribution $\epsilon(y)$ across the monitored section can be written:

$$\varepsilon(y) = \frac{1}{L_{IP}} u(y) = \frac{1}{L_{IP}} (\bar{d} + \varphi y) \quad (6)$$

Based on these definitions, it is now possible to enhance the representation of the slice deformation by relaxing the assumption of perfect bond between steel and concrete. This can be done by assuming that the deformation of the steel component is due partly to the bar elongation and partly to the slip between the bar and the concrete. This is expressed in the following form:

$$\begin{cases} \bar{d} = \bar{d}_c = \bar{d}_{s+a} = \bar{d}_s + \bar{d}_a \\ \varphi = \varphi_c = \varphi_{s+a} = \varphi_s + \varphi_a \end{cases} \quad (7)$$

in which the slice axial deformation \bar{d} and the slice rotation φ are expressed as sum of two contributions, one due to the rebar deformation (subscript s), the other to the anchorage slip (subscript a).

From Eq. (7), the concrete strain is the same as in Eq. (6)

$$\varepsilon(y_c) = \frac{1}{L_{IP}} (\bar{d}_c + \varphi_c y_c) = \bar{\varepsilon} + \kappa y_c \quad (8)$$

whereas the steel strain becomes

$$\varepsilon_{s+a} = \frac{1}{L_{IP}} (\bar{d}_s + \varphi_s y_s) + \frac{1}{L_{IP}} (\bar{d}_a + \varphi_a y_s) \quad (9)$$

in which the first term represents the strain of the steel bar in the slice and the second is the contribution of the bond-slip. Therefore

$$\varepsilon_{s+a} = \varepsilon_s + \frac{1}{L_{IP}} u_a = \varepsilon_s + \varepsilon_a \quad (10)$$

in which ε_a should be regarded as a strain-equivalent contribution of the anchorage pullout, condensed at the fiber level through the length L_{IP} of the integration point. In other words, the total steel fiber elongation is given by the sum of the rebar deformation and anchorage pullout. Compatibility is maintained between the concrete strain and the total steel fiber elongation ($\varepsilon_c = \varepsilon_{s+a}$), while concrete and steel strains are different ($\varepsilon_c \neq \varepsilon_s$). This procedure is illustrated in Figure 1 for the case of a slice with axial deformation only and no curvature.

The fiber section state determination is identical to that presented in Spacone et al. (1996a). Given the section deformations $\bar{\varepsilon}$ and κ , find the corresponding section forces and stiffness. The fiber strains $\varepsilon(y) = \bar{\varepsilon} + \kappa y$ are computed first. Based on the new strain field the fiber stresses and tangent moduli are computed. They are then integrated over the cross section to yield the section forces and stiffness.

The main difference introduced by the new approach concerns the fiber response. While the concrete strain is directly computed from Eq. (8), the steel strain determination is more involved because Eq. (9) yields the total steel response ε_{s+a} . A specific procedure has been developed to compute the rebar deformation ε_s and average anchorage slip ε_a corresponding to ε_{s+a} .

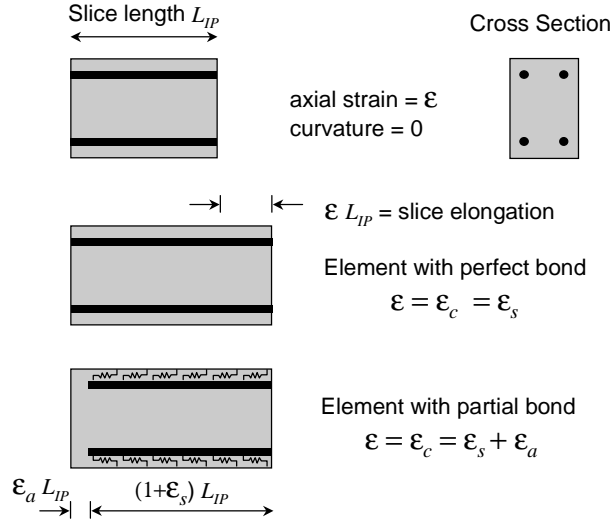


Figure 1. Slice response to axial deformation only: perfect bond vs. partial bond

Steel Bar State Determination

The steel fiber state determination computes the rebar stress and stiffness corresponding to the total strain $\epsilon_{s+a} = \epsilon_s + u_a / L_{IP}$. The system represents a steel rebar of length L_{IP} plus the bar anchorage of length L_a . In this case the anchorage length L_a extends outside the element in the beam-column joint. The rebar is modeled with a simple bar element, whose constitutive law is that of a reinforcing bar. The embedded bar is modeled by a series of rebars with continuous bond embedded in concrete, following the approach proposed by Monti et al. (1997a and b). The following linearized constitutive laws are used:

$$\sigma_s = E_s \epsilon_s \quad \begin{Bmatrix} \sigma_a \\ \mathbf{0} \end{Bmatrix} = \begin{bmatrix} k_{aa} & \mathbf{k}_{an} \\ \mathbf{k}_{na} & \mathbf{k}_{nn} \end{bmatrix} \begin{Bmatrix} u_a \\ \mathbf{u}_n \end{Bmatrix} \quad (11)$$

in which the anchorage dof's have been split into the anchorage displacement u_a and the displacements \mathbf{u}_n of the other n nodes along the anchorage length. The $\mathbf{0}$ vector in the stress vector indicates that the bar is subjected only to an end stress σ_a , while all other dof's have no applied stress. The last node n at the anchorage tip is therefore unrestrained. The value of n depends on the number of elements used to discretize the length L_a of the anchorage zone. A study on the optimal number of elements can be found in Monti et al. (1997a).

The following deformation vector \mathbf{e} is associated with each fiber

$$\mathbf{e} = \frac{1}{L_{IP}} \{ L_{IP} \epsilon_s \quad u_a \quad \mathbf{u}_n \}^T \quad (12)$$

Using this notation the strain in the "steel fiber + anchorage" system ($s+a$) given by Eq. (10) is written

$$\epsilon_{s+a} = \mathbf{m}^T \mathbf{e} \quad (13)$$

in which $\mathbf{m} = \{1 \quad 1 \quad \mathbf{0}\}^T$. A steel fiber stress vector \mathbf{s} is also defined

$$\mathbf{s} = \{ \sigma_s \quad \sigma_a \quad \mathbf{s}_n^U \}^T \quad (14)$$

in which \mathbf{s}_n^U is the stress unbalance vector at the nodes along the anchorage length. This unbalance is included because of the nonlinearity of the problem. During the solution process, it is likely to have $\mathbf{s}_n^U \neq \mathbf{0}$. When the anchorage solution is reached $\mathbf{s}_n^U \rightarrow \mathbf{0}$.

Due to the series arrangement of steel and anchorage expressed by Eq. (10) the steel fiber and the anchorage have the same applied stress

$$\sigma_{s+a} = \sigma_s = \sigma_a \quad (15)$$

which allows rewriting the stress vector of Eq. (14) as

$$\mathbf{s} = \mathbf{m} \sigma_{s+a} + \left\{ 0 \quad 0 \quad \mathbf{s}_n^U \right\}^T \quad (16)$$

The two local constitutive relationships (11) are grouped in a single expression

$$\mathbf{s} = \mathbf{K} \mathbf{e} = L_{IP} \begin{bmatrix} E_s/L_{IP} & 0 & \mathbf{0} \\ 0 & k_{aa} & \mathbf{k}_{an} \\ \mathbf{0} & \mathbf{k}_{na} & \mathbf{k}_{nn} \end{bmatrix} \mathbf{e} \quad (17)$$

The stiffness matrix in Eq. (17) can be built using the virtual force principle. The virtual force principle can then be written in the following form:

$$\delta \sigma_{s+a} \varepsilon_{s+a} = \delta \mathbf{s}^T \mathbf{e} \quad (18)$$

The virtual variation of the stress vector should be in equilibrium ($\delta \mathbf{s}_n^U = \mathbf{0}$), and is given by

$$\delta \mathbf{s} = \mathbf{m} \delta \sigma_{s+a} \quad (19)$$

Upon substitution of (19) into (18) and after elimination of the virtual variation $\delta \sigma_{s+a}$ from the standard argument of arbitrariness, Eq. (18) is written

$$\varepsilon_{s+a} = \mathbf{m}^T \mathbf{e} = \mathbf{m}^T \mathbf{K}^{-1} \mathbf{s} = \mathbf{m}^T \mathbf{F} \mathbf{s} \quad (20)$$

in which Eq. (17) has been substituted. The flexibility matrix \mathbf{F} is given by

$$\mathbf{F} = \mathbf{K}^{-1} = \frac{1}{L_{IP}} \begin{bmatrix} L_{IP}/E_s & 0 & \mathbf{0} \\ 0 & f_{aa} & \mathbf{f}_{an} \\ \mathbf{0} & \mathbf{f}_{na} & \mathbf{f}_{nn} \end{bmatrix} \quad (21)$$

Upon substitution of (16) into (20), one obtains

$$\varepsilon_{s+a} = \mathbf{m}^T \mathbf{F} \mathbf{m} \sigma_{s+a} + \mathbf{m}^T \mathbf{F} \begin{Bmatrix} 0 \\ 0 \\ \mathbf{s}_n^U \end{Bmatrix} \quad (22)$$

and Eq. (22) is inverted to yield

$$\sigma_{s+a} = E_{s+a} (\epsilon_{s+a} - \epsilon_n^U) \quad (23)$$

in which E_{s+a} is the stiffness of the steel plus bond fiber

$$E_{s+a} = [\mathbf{m}^T \mathbf{F} \mathbf{m}]^{-1} = \left(E_s^{-1} + \frac{1}{L_{IP}} f_{aa} \right)^{-1} \quad (24)$$

and the strain

$$\epsilon_n^U = \mathbf{m}^T \mathbf{F} \begin{Bmatrix} 0 \\ 0 \\ \mathbf{s}_n^U \end{Bmatrix} = \frac{1}{L_{IP}} \mathbf{f}_{an} \mathbf{s}_n^U \quad (25)$$

represents the residual strain due to the unbalanced forces along the anchorage length. As the solution approaches convergence, $\epsilon_n^U \rightarrow 0$. The result of this procedure is schematically shown in Figure 2.

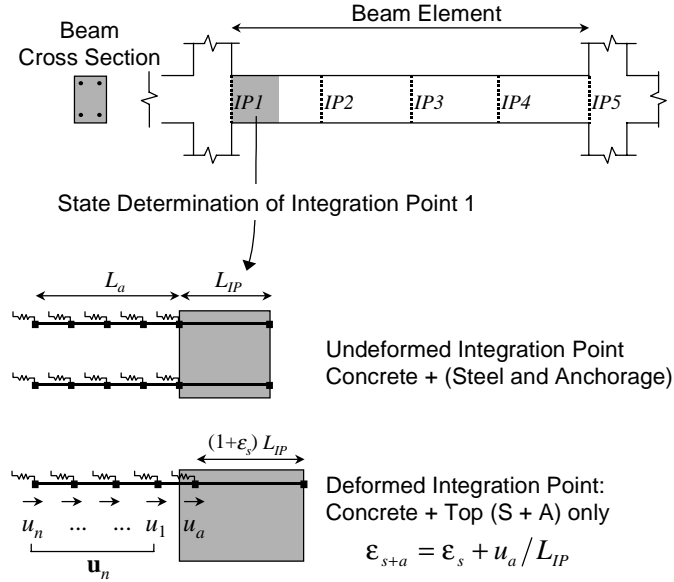


Figure 2 Steel bar state determination including anchorage slip

COMPARISON WITH EXPERIMENTAL RESULTS

In this section a comparison with an experimental test performed by Saadatmanesh et al. (1996) is performed. The test was conducted on a scaled-down circular reinforced concrete bridge column, designed according to obsolete seismic codes, with insufficient development lengths for the rebars anchored in the footing. Ready-mixed concrete with $f'_c = 36.5$ MPa and steel with measured yield strength of 358 MPa were used. The diameter of the column was 305 mm and the longitudinal reinforcement was 14 bars of 13-mm diameter, resulting in a reinforcement ratio of 2.48%. Transverse confinement was provided by steel wire hoops of diameter 3.5 mm and spaced at 89 mm throughout the entire height of the column. The average yield stress for these wires was 301 MPa. In the specimen (denoted as C-1) the longitudinal reinforcement of the column was extended into the footing using starter bars that were lapped with the main longitudinal reinforcement of the column over a length of 20 bar diameters (254 mm). In the test an axial load of 445 kN was first applied to the column, followed by cyclic lateral displacements applied at the top of the column in both positive and negative directions according to the scheme: $1u_y$, $1.5u_y$, $2u_y$, $3u_y$, where u_y is the yield displacement. At each displacement

level, two cycles were performed. Figure 3a shows the hysteresis loops for the experimental response of the circular column C-1 with lap splice. (Saadatmanesh et al. (1996)). The weak bond response already observed in the previous section characterizes the test. After the first cycle to $u=1.5u_y$, there is a rapid degradation of the response due to progressive failure of the lapped reinforcement due to slip. In addition, it is noted that the cycles show significant pinching, with extremely reduced dissipation capacity. Figure 3b presents two numerical simulations of the experimental test. The first was performed with the fiber element model with perfect bond presented in Spacone et al. (1996a), the second uses the model proposed in this paper that includes bond-slip of the rebars. The differences in the prediction are remarkable, the most evident regarding the dissipation capacity, which is of paramount importance in seismic analyses. The model with no bond-slip predicts fuller cycles, which are far from being similar to those obtained in the test. The prediction obtained with the new model is similar to the experimental result. Another remarkable difference regards the prediction of the peak load cyclic degradation. The response obtained with the new model shows a decay that is very similar to the experimental case, thanks to its capacity of tracing the bond-damage penetration into the anchorage. A more sophisticated cyclic degradation rule in the bond-slip constitutive law would lead to further enhancements in the prediction capabilities of the proposed model. Finally, it is important to point out the complexity of the simulation in which the reinforcing bars all have different responses, since the steel is distributed along the perimeter of the circular reinforced concrete section and all the rebars have different strains.

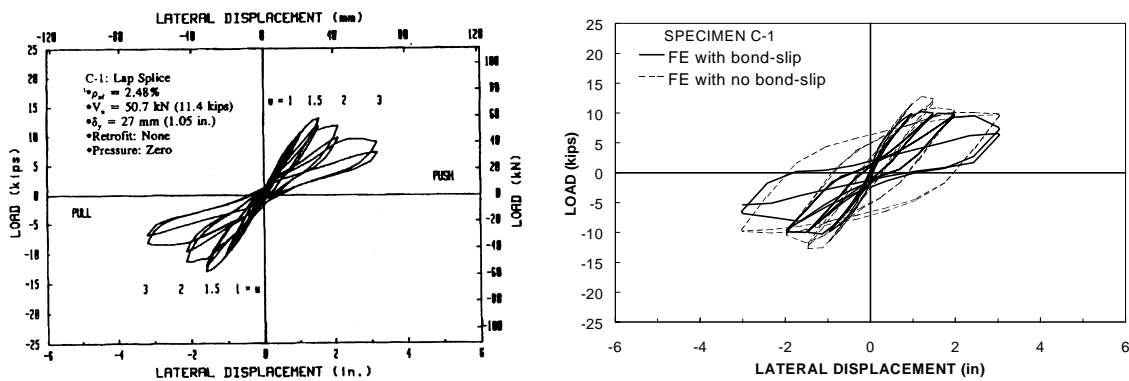


Figure 3 Comparison between experimental test (left) from Saadatmanesh et al. (1996) and numerical simulation (right) with and without bond-slip

CONCLUSIONS

A fiber beam element that includes bond-slip of the reinforcing bars has been presented. The formulation is derived from the force-based fiber beam element proposed by Spacone et al. (1996a), with the insertion of bar element with continuous bond developed by Monti et al. (1997a and b).

The response of the beam element is obtained through the weighted integration of the responses of the monitored sections along the element. The fiber section response is computed by adding the contributions of all the concrete and steel fibers in which the section is subdivided. In the proposed beam element, the steel fiber state determination is modified to account for the bond-slip of the rebars. In the original model, the steel stress and stiffness are calculated directly from the steel constitutive law, based on the strain pertaining to the fiber. In the new model, the stress and stiffness of each steel fiber are obtained as the response of a bar that crosses the section under consideration and is anchored in the concrete. The end slip can also be computed, in order to give an estimate of the crack width. The implementation is simple and requires minor modifications to the structure of the original fiber beam element, provided a modular organization of the element routines is followed.

Since the new formulation affects the fiber section model only and does not affect the overall element state determination, the proposed fiber section model with bond-slip in the steel rebars can be implemented in any displacement-based or force-based that uses a fiber section discretization. In the present form the model is implemented in a force-based element that is linked to the general purposed Finite Element program FEAP (Taylor, 1998).

Because each steel rebar in the cross section is monitored separately, the proposed model applies to cross sections of any shape. For the same reason, the model can be applied to both uniaxial and biaxial bending problems.

A comparison between experimental data and numerical simulations has been presented. This study has shown that the results obtained with the proposed model correlate well with the experimental data, while the original fiber model with perfect bond largely overestimates the hysteretic energy dissipated during the loading cycles.

The proposed model can be applied to the study of reinforced concrete frames. For new structures it will provide a more realistic prediction of the initial stiffness than that obtained from the fiber model with perfect bond. For older structures with insufficient anchorage lengths or lap splices it can realistically account for bond deterioration and failure under both static and dynamic loading conditions. Cases will be examined, where the anchorage length is insufficient, such as beam-column joints. This will be the basis for further studies on complex structural systems where the slippage between two framing elements will be accounted for.

REFERENCES

- Monti, G., Filippou, F.C., and Spacone, E. (1997a). "Finite element for anchored bars under cyclic load reversals." *Journal of Structural Engineering, ASCE*, 123(5), 614-623.
- Monti, G., Filippou, F.C., and Spacone, E. (1997b). "Analysis of hysteretic behavior of anchored reinforcing bars." *ACI Structural Journal*, May-June, 94(3), 248-261.
- Saadatmanesh, H., Ehsani, M.R., and Jin, L. (1996). "Seismic strengthening of circular bridge pier models with fibre composites." *ACI Structural Journal*, Nov-Dec, 93(6), 639-647.
- Spacone, E., Filippou, F.C., and Taucer, F.F. (1996a). "Fibre beam-column model for nonlinear analysis of R/C frames. Part I: formulation." *Earthquake Engineering and Structural Dynamics*, 25, 711-725.
- Spacone, E., Filippou, F.C., and Taucer, F.F. (1996b). "Fibre beam-column model for nonlinear analysis of R/C frames. Part I: applications." *Earthquake Engineering and Structural Dynamics*, 25, 727-742.
- Taylor, R.L. (1998). "FEAP: A Finite Element Analysis Program. User Manual: Version 7.1" Department of Civil and Environmental Engineering, University of California, Berkeley.